RESEARCH ARTICLE (Open Access)

Region of Interest (ROI) Compute Volume in Bilayer Titanium and Polycaprolactone Scaffolds used for Osteochondral Regeneration: A CT Study in Sheep Model

TAULANT GOGA[1*], BLEDAR GOXHA[1], ANTONIO CROVACE[2], ERINDA LIKA[1], FRANCESCO STAFFIERI[2], ALTIN METALLA[1], ALBERTO MARIA CROVACE[3]

[1]Faculty of Veterinary Medicine, Agricultural University of Tirana, 1025 Tirana, Albania;

[2]Department of Precision and Regenerative Medicine and Ionian Area, University of Bari "ALDO MORO", 70010 Bari, Italy;

[3]Department of Veterinary Medicine, University of Sassari, 07100 Sassari, Italy.

*Corresponding author; E-mail: tgoga@ubt.edu.al

Abstract

Osteochondral defects, involving damage to both articular cartilage and subchondral bone, present significant challenges due to their limited spontaneous healing capacity and the risk of progression to osteoarthritis. Biomaterial scaffolds play a crucial role in tissue engineering by providing three-dimensional frameworks that support cell attachment and direct the formation of new tissue, with or without the incorporation of growth factors and biological cells. This study evaluated the regenerative potential of bilayer porous scaffolds composed of polycaprolactone (PCL) and titanium–polycaprolactone (TiPCL) in a sheep model, with the sample size of 8 sheep per each group. Using computed tomography (CT) imaging and region-of-interest (ROI) analysis, we quantitatively assessed volumetric and densitometric parameters over a 12-month period at four time points: immediately post-implantation (T0), and at 3 (T3), 9 (T9), and 12 (T12) months. The TiPCL group demonstrated significantly higher maximum (3685 - 4000 HU) and mean (1280 – 1472 HU) values, greater standard deviation (889 – 932 HU), and increased total HU across most time points compared to both the PCL and control (CNTR) groups, indicating enhanced mineralization and structural heterogeneity. In contrast, the PCL group exhibited moderate increases in densitometric parameters, while the CNTR group showed minimal changes, suggesting limited spontaneous healing. These findings underscore the superior osteogenic capacity of TiPCL scaffolds, highlighting their potential in promoting effective bone regeneration in osteochondral defects.

Keywords: Region of Interest; Osteochondral defect; Bilayer scaffolds, Titanium, Polycaprolactone.

1. Introduction

Osteochondral defects involve damage to both the articular cartilage and the underlying subchondral bone, and such lesions often do not heal spontaneously, making them a significant risk factor for eventual osteoarthritis[1,2]. These defects are difficult to manage because cartilage and subchondral bone have distinct structures and limited healing capacity, yet function as a single unit, so damage to the bone impairs cartilage repair and often results in fibrous scar tissue rather than functional cartilage[3,4].

In the absence of effective intervention, these defects fail to heal on their own and may progress to degenerative joint disease, with loss of the osteochondral unit impairing joint function and leading to chronic pain and disability, following the need for regenerative solutions[5,6]. Conventional surgical treatments (e.g. microfracture, osteochondral autografts, allografts, or autologous chondrocyte implantation) provide only partial and temporary relief,

*Corresponding author: Taulant Goga; E-mail: tgoga@ubt.edu.al
(Accepted for publication 24.03.2026)
***ISSN**: 2218-2020,*

with limitations especially in restoring the cartilage component of the lesions[7]. In response, osteochondral tissue engineering has emerged as a regenerative strategy that combines principles of biology, materials science, and bioengineering to repair the osteochondral unit[8]. This approach aims to promote the integrated regeneration of both cartilage and bone, for example through scaffold-free cell constructs or multiphasic scaffolds that mimic the native osteochondral structure[9].

Biomaterial scaffolds are a critical component of tissue engineering, serving as three-dimensional frameworks that provide structural support for cell attachment and guide new tissue formation, with or without the incorporation of growth factors and biological cells[10]. A wide range of biomaterials have been explored for scaffold design, including natural polymers (e.g. collagen), synthetic polymers (e.g. polycaprolactone or polylactic acid), bioactive ceramics (e.g. hydroxyapatite), and metals like titanium[11]. Each class of material offers distinct advantages and limitations. Synthetic biodegradable polymers such as polycaprolactone (PCL) are widely used due to their good biocompatibility and degradability[10]. However, PCL by itself degrades slowly in vivo and has relatively poor hydrophilicity and osteoinductive capacity, which can limit cell adhesion and bone formation[12,13]. Its slow-degrading, semi-crystalline structure enables scaffolds to provide structural support during bone repair. 3D-printed PCL scaffolds enriched with 20% bioactive fillers (hydroxyapatite, β-tricalcium phosphate, or bioglass) promote significant bone ingrowth in a critical-size sheep femoral condyle defect within 6 weeks[13]. In contrast, titanium (Ti) is a mechanically robust, biocompatible metal that is often fabricated as a porous scaffold to improve osteointegration. Porous Ti scaffolds (with ~60–70% porosity) in combination with Polycaprolactone (TiPCL) can achieve stiffness comparable to cancellous bone and support early bone cell ingrowth, albeit as a non-resorbable implant with limited intrinsic osteogenic activity[8,14,15]. Such combinations aim to provide strong mechanical support from the metal component while maintaining a bioactive surface for cell adhesion and cartilage regeneration from the polymer/collagen component. These advances in scaffold design, including biphasic and triphasic scaffold architectures, seek to regenerate both subchondral bone and articular cartilage concurrently[16].

Evaluating the performance of novel osteochondral scaffolds in a biologically relevant setting is essential for translational research. Large-animal models, particularly sheep, are widely used in preclinical osteochondral repair studies because they closely approximate human joint size, loading conditions, and biological responses[17]. In this study, a sheep model with standardized critical-size osteochondral defects created in the medial femoral condyle was employed to assess long-term scaffold performance. Such models enable the evaluation of implant behavior, tissue regeneration, and scaffold stability under physiological weight-bearing conditions over extended follow-up periods.

Advanced imaging techniques, particularly X-ray computed tomography (CT), enable non-destructive, three-dimensional evaluation of new tissue formation inside the osteochondral lesion treated by different biomaterials. High-resolution CT can scan excised specimens to produce 3D reconstructions of the healing osteochondral defect, allowing quantification of the newly formed bone volume and architectural parameters within the scaffold[8,18]. To enable non-invasive longitudinal assessment of bone regeneration in vivo, a region of interest (ROI)-based analysis was performed using CT. Quantitative CT allows reliable evaluation of mineralized tissue formation within osteochondral defects, as Hounsfield unit (HU) values correlate with bone mineral density[19,20]. For each implanted scaffold, serial CT scans were acquired and a standardized ROI encompassing the defect area was defined. This approach enabled the calculation of multiple volumetric and density-related parameters, including mineralized tissue volume and HU-based metrics (Volume, Min, Max, Mean, Sdev, and Total HU values). Among these parameters, the mean ROI HU value represents a particularly robust indicator of bone regeneration, as it reflects the overall mineral density of newly formed tissue and has been identified as a key metric for identifying scaffold performance in osteochondral repair studies[21].

The aim of this study was to compare the osteochondral regenerative performance of bilayer porous polycaprolactone (PCL) and bilayer porous titanium–polycaprolactone (TiPCL) scaffolds using CT-derived ROI metrics over a 12-month follow-up period in a sheep model. By integrating long-term in vivo experimentation with quantitative ROI-based CT analysis, this study seeks to objectively identify the scaffold that provides superior osteochondral repair

and to support the development of more effective biomaterial strategies for clinical translation.

2. Material and Methods

The animals selected for the experimental study were identified and acclimatized for a period of 30 days before surgery. Twenty-four adult female sheep, all in good health, underwent ultrasonographic examination to exclude pregnancy and received routine anthelmintic treatment (Ivomec®, Boehringer Ingelheim; 1 ml/50 kg body weight). Preoperative orthopedic evaluations, including clinical examination and radiographs, were performed to exclude pre-existing musculoskeletal pathology and to assess the integrity of the condylar region of the right femur.

2.1. Experimental design and biomaterial groups

After clinical screening, the sheep were randomly allocated into three experimental groups and one control group according to the implanted biomaterial.

• Control group (CNTR): In this group were included 8 sheep and the osteochondral defect was created but left untreated to allow spontaneous healing.

• Bilayer porous PCL group: In this group were included 8 sheep and the osteochondral defects was treated with a bilayer porous PCL scaffold designed to mimic native osteochondral architecture through a dual-layer configuration supporting both cartilage and subchondral bone regeneration.

• Bilayer porous TiPCL group: In this group were included 8 sheep and the osteochondral defect was treated with a bilayer porous TiPCL composite scaffold, combining the mechanical strength and osteoconductive properties of titanium with the biodegradability and flexibility of polycaprolactone to enhance osteointegration.

Bilayer PCL scaffolds were fabricated via additive manufacturing to generate a highly interconnected porous architecture that optimizes cell infiltration, vascularization and nutrient diffusion. The bilayer TiPCL composite scaffolds were produced through selective laser melting followed by polymer infiltration to achieve mechanical stability and biofunctional surfaces. These fabrication approaches have been shown to promote osteogenic differentiation and tissue integration in previous studies.

2.2. Surgical procedure and postoperative care

In each sheep, an experimental osteochondral lesion measuring 15 mm in diameter and 10 mm in depth was created on the medial condyle of the right femur using a calibrated surgical drill. Scaffold implantation was performed by the same surgical team, ensuring precise positioning and press-fit fixation within the defect site. All surgical procedures were conducted under sterile conditions by the same experienced team, using a combination of general and spinal anesthesia. Postoperative analgesia and antibiotic prophylaxis were administered according to standard veterinary protocols.

After surgery, animals were housed at the Veterinary Clinics and Animal Production Section of the Department of Precision and Regenerative Medicine and Ionian Area (DiMePRe-J), University of Bari, Italy. Daily clinical monitoring included evaluation of food intake, body weight, urine and feces production, rectal temperature, wound healing and behavioural patterns.

2.3. Computed tomography and image analysis

To assess osteochondral regeneration and scaffold integration, all sheep underwent CT imagings at predefined postoperative time points. Scans were performed using a GE BrightSpeed 16-slice CT scanner with the following parameters: helical mode, slice thickness of 1.25 mm, tube voltage of 120 kVp, tube current of 200 mA, pitch of 0.93 and bone convolution kernel. Limbs were positioned cranio-caudally and scanned from the distal femoral diaphysis to the proximal tibial diaphysis.

Multiplanar reconstructions were generated using Aycan OsiriX Pro® software, and quantitative image analyses were performed using the HOROS imaging platform. Volumetric and densitometric parameters were extracted using the ROI Compute Volume function to enable quantitative three-dimensional evaluation of the osteochondral defect treated with implanted scaffolds. Volume (cm^3) quantified the total size of the analyzed region, reflecting tissue formation within the defect site. Mean (HU) represented the average radiodensity and served as an indirect indicator of mineralized tissue deposition and bone regeneration. Minimum and maximum HU values described the density range within the ROI, allowing identification of areas with lower or higher degrees of mineralization. Standard deviation (Sdev) assessed the variability of HU values, providing insight into the structural homogeneity of the regenerating tissue. Finally, total

HU represented the cumulative radiodensity of all voxels within the ROI, integrating both volumetric and density information to characterize the overall regenerative response to the implanted biomaterials. In this study was taken in consideration for evaluation only 3D volumetric reconstruction (ROI Compute Volume) values. A total of 48 tomographic images were obtained in this study, resulting from the evaluation of 4 sheep at each time point (0, 3, 9, and 12 months) in each study group (CNTR, PCL, and TiPCL). T0 displays CT images immediately following implantation, T3 displays CT images three months later, T9 displays CT images nine months later, and T12 displays CT images twelve months later.

2.4. Statistical analysis

Statistical analyses were performed using R software (version 20226.01.0-392). Data are presented as mean ± standard deviation (SD). To assess the effects of treatment groups (CNTR, PCL, TiPCL) and time points (T0, T3, T9, T12) on the measured variables, a two-way analysis of variance (ANOVA) was employed. This approach allows for the evaluation of the main effects of each independent variable and their potential interaction on the dependent variables[22]. Prior to conducting ANOVA, assumptions of normality and homogeneity of variances were verified using the Shapiro-Wilk test and Levene's test, respectively. When significant main effects or interactions were identified ($p < 0.05$), post hoc analyses were performed using Tukey's Honestly Significant Difference (HSD) test. This method controls the family-wise error rate and is appropriate for all pairwise comparisons among group means[23]. Two-way ANOVA is widely recommended for factorial experimental designs as it enables the detection of interaction effects between independent variables, thereby providing a more comprehensive interpretation of treatment-related changes over time. Due to ethical and logistical constraints associated with large-animal studies, a formal a priori power analysis was not performed, resulting in a limited sample size of 8 individuals per group.

3. Results and Discussion

All data included in this study were successfully analyzed with respect to the HU values of the ROI Compute Volume parameters selected for this investigation. Table 1 presents the mean and standard deviation (SD) values, expressed in HU, for all ROI Compute Volume parameters obtained from the three-dimensional reconstruction of the implanted scaffolds. These data illustrate how the values change over time (T0, T3, T9, and T12) across the three study groups: CNTR, bilayer porous PCL and bilayer porous TiPCL.

Table 1 Quantitative CT analysis showing HU measurements — including volume, minimum, maximum, mean, standard deviation, and total values — recorded at T0, T3, T9, and T12 for the CNTR, PCL and TiPCL groups

Parameter	***Group***	***T0***	***T3***	***T9***	***T12***
Volume (HU)	CNTR	0,6277 ± 0,18	1,0228 ± 0,14	0,7050 ± 0,07	0,8557 ± 0,07
	PCL	0,7155 ± 0,03	0,9950 ± 0,29	0,9003 ± 0,20	0,8225 ± 0,38
	TiPCL	0,8479 ± 0,04	0,7898± 0,07	0,6823 ± 0,20	1,2492 ± 0,21
Min (HU)	CNTR	-1208,25 ± 230,57	-177,5 ± 14,71	-156,25 ± 48,32	-95,25 ± 24,34
	PCL	-828,25 ± 193,50	-117,75 ± 183,05	-52,5 ± 61,81	-41 ± 29,09
	TiPCL	-862,5 ± 464,77	-574,25 ± 453,05	-373,25 ± 23,94	-333,5 ± 145,31
Max (HU)	CNTR	1026 ± 242,07	1661,5 ± 119,51	1472,5 ± 94,37	1651,75 ± 104,46
	PCL	1069,75 ± 95,28	1284,5 ± 166,86	1357,25 ± 84,70	1370,5 ± 120,48
	TiPCL	3973,75 ± 52,50	3685,25 ± 101,74	3820 ± 280,67	4000 ± 0,00
Mean (HU)	CNTR	-61,38 ± 177,77	270,29 ± 101,88	479,60 ± 1,15	465,98 ± 7,48
	PCL	112,22 ± 24,39	279,076 ± 89,53	299,92 ± 21,72	402,98 ± 43,85
	TiPCL	1367,17 ± 143,23	1284,88 ± 89,55	1471,78 ± 102,65	1280,79 ± 204,42
Sdev (HU)	CNTR	346,77 ± 133,07	312,92 ± 40,36	318,13 ± 7,47	372,17 ± 2,11
	PCL	254,97 ± 27,10	299,04 ± 69,04	285,08 ± 20,68	365,22 ± 42,58
	TiPCL	917,81 ± 76,74	888,78 ± 29,71	903,85 ± 73,97	932,30 ± 18,68
Total (HU)	CNTR	12523,5 ± 507413,05	3191012,5 ± 1089121,36	1568190,75 ± 413577,62	2419027,0 ± 144090,47

	PCL	234216,75 ± 54917,96	818967,75 ± 380783,34	742548,0 ± 72204,08	1205927,75 ± 298533,05
	TiPCL	3286602,25 ± 390357.9	2551310,0 ± 703191,26	2803629,0 ± 1476252,0	6281571,5 ± 684292,12

Volume values increased in both CNTR and bilayer PCL at T3, followed by a decline at T9 and stabilization by T12, suggesting a transient volumetric expansion. In contrast, bilayer TiPCL showed an initial decrease from baseline to T9 before rising markedly at T12, reaching the highest volume among all groups. Minimum HU values became progressively less negative in CNTR and bilayer PCL throughout the study, indicating a reduction in very low-density components; however, bilayer TiPCL maintained substantially lower minimum values at all time points, implying the persistent presence of less dense tissue regions. Maximum HU values remained relatively similar between CNTR and bilayer PCL, fluctuating moderately around 1000 – 1650 HU, whereas bilayer TiPCL consistently exhibited markedly higher maxima (approximately 3 700–4 000 HU), reflecting the presence of highly dense structures within this group due to presence of titanium.

Mean HU values further highlight these differences: CNTR transitioned from slightly negative values at baseline to progressively higher positive values, while bilayer PCL demonstrated a steady increase across time. Bilayer TiPCL maintained considerably higher mean HU values than the other groups at every time point, indicating overall greater tissue density. The standard deviation of HU was consistently largest in bilayer TiPCL, suggesting pronounced heterogeneity in tissue composition, whereas CNTR and bilayer PCL showed lower variability with only modest increases by 12 months. Total HU followed a similar pattern, with bilayer TiPCL displaying the greatest cumulative density and a notable rise by T12. Also, CNTR group showed a strong increase over time despite large variability, while bilayer PCL exhibited a more gradual upward trend. These findings indicate that although CNTR and bilayer PCL experience moderate densification and relatively stable structural characteristics, bilayer TiPCL exhibits much higher density, greater heterogeneity, and more pronounced cumulative changes over the 12-month period.

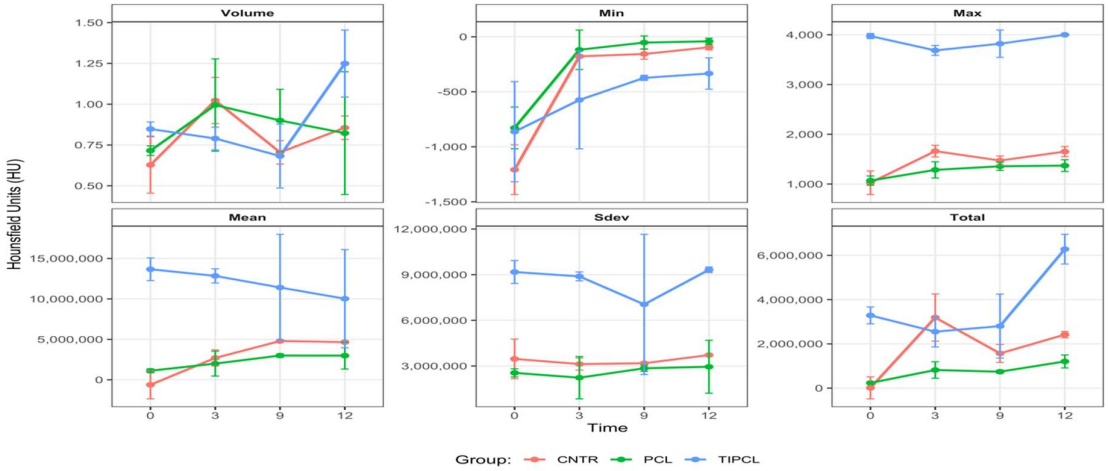

Figure 1. Longitudinal comparison of Hounsfield Unit (HU)–based metrics across time points (0, 3, 9, and 12) for the CNTR, PCL, and TIPCL groups. Panels display Volume, Minimum (Min), Maximum (Max), Mean, Standard Deviation (Sdev), and Total values, with error bars indicating variability.

The temporal evolutions of all volumetric and densitometric parameters derived from ROI Compute Volume analysis are illustrated in Figure 1. Volume values showed a generally stable trend across groups, with a slight increase at later time points, particularly in the bilayer TiPCL group. Min HU values increased

progressively in all groups, indicating a reduction in low-density regions over time. The bilayer TiPCL group consistently exhibited markedly higher max HU values compared to CNTR and bilayer PCL, suggesting enhanced mineralization. Similarly, mean HU values were substantially greater in the TiPCL group throughout the study period, while CNTR and bilayer PCL demonstrated more gradual increases. Sdev remained relatively stable, although higher variability was observed in bilayer TiPCL, reflecting heterogeneous tissue formation. Total HU values increased over time, with the most pronounced rise detected in the bilayer TiPCL group at T12, indicating a stronger overall mineralized tissue response compared to the other groups.

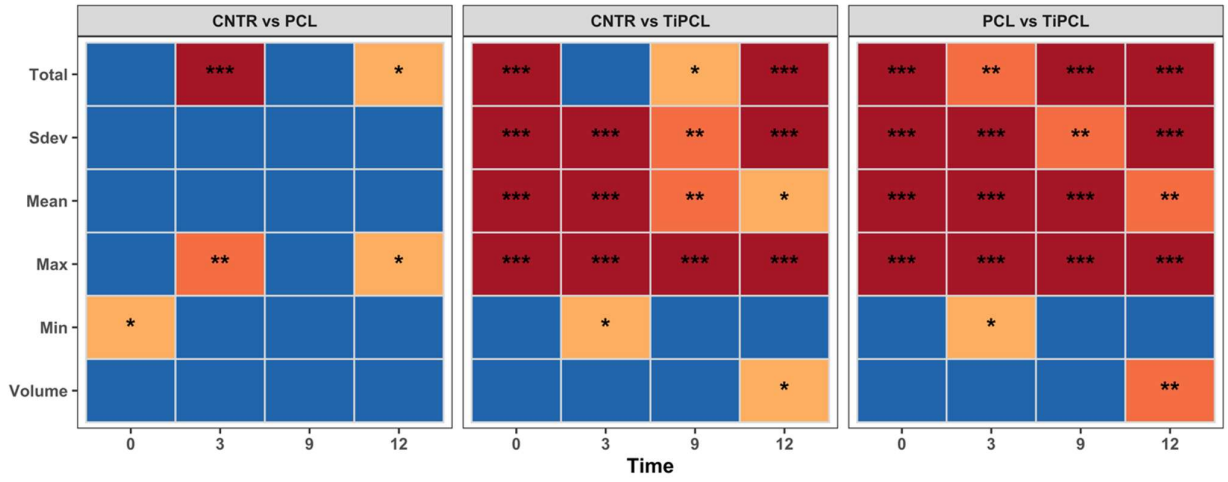

Figure 2. Time-Dependent Pairwise Statistical Comparisons Between Experimental Groups.

Figure 2 presents all statistically significant comparisons between groups over time for all ROI Compute Volume parameters. Statistical significance is indicated as follows: * for p-values < 0.05, ** for p-values < 0.01, and *** for p-values < 0.001. The comparison between the CNTR and bilayer TiPCL groups revealed statistically significant differences for nearly all evaluated parameters, particularly for Max, Mean, SD, and Total values, across most time points, indicating a sustained divergence between these groups throughout the observation period. Similarly, the bilayer PCL versus bilayer TiPCL comparison demonstrated highly significant differences in the majority of parameters, with statistical significance evident as early as T0 and persisting through T12. This consistent separation suggests that bilayer TiPCL promotes structural changes that are clearly distinguishable from those associated with bilayer PCL.

In contrast, differences between CNTR and bilayer porous PCL were less consistent and appeared to be parameter-dependent. Statistically significant differences were mainly observed at intermediate and later time points for Total and Max values, whereas the remaining parameters showed limited or no significant separation. This pattern may reflect a more gradual divergence between these groups over time. These findings underscore the strong influence of treatment type on the evaluated imaging parameters and suggest that the bilayer TiPCL condition induces the most pronounced structural changes during the study period. The quantitative analysis of ROI Compute Volume parameters in this study provides compelling evidence of the differential regenerative capacities of the evaluated scaffolds over a 12-month period. Importantly, the bilayer TiPCL group exhibited superior performance across multiple densitometric metrics, including significantly higher maximum and mean HU values, as well as elevated total HU, compared to both the CNTR and bilayer PCL groups. These findings suggest enhanced mineralization and scaffold integration associated with the incorporation of titanium into the bilayer PCL scaffold.

The continuous increase in maximum HU values seen in the bilayer TiPCL group indicates the presence of highly mineralized tissue, which is consistent with the osteoconductive properties of titanium-based scaffolding. This is consistent with prior research showing that metallic components in scaffolds can dramatically increase bone regrowth[24].

In contrast, the bilayer PCL group showed a more gradual increase in densitometric parameters, reflecting its known biocompatibility and biodegradability but limited osteoinductive capacity. This observation is consistent with literature indicating that while bilayer PCL scaffolds support cell proliferation and tissue ingrowth, their lack of bioactivity necessitates modification or combination with other materials to enhance bone regeneration[25].

The CNTR group exhibited the least pronounced changes in densitometric values over time, underscoring the importance of scaffold intervention in promoting bone regeneration. The minimal variation in HU values suggests limited spontaneous healing in the absence of a scaffold, highlighting the critical role of scaffold materials in facilitating tissue repair.

The observed differences in SD of HU values among the groups further elucidate the heterogeneity of tissue formation. The higher SD in the bilayer TiPCL group may reflect a more complex tissue remodeling process, potentially due to the interplay between the titanium component and the surrounding biological environment. This complexity could be indicative of active bone remodeling and maturation processes facilitated by the scaffold's composition.

These findings underscore the significant impact of scaffold composition on bone regeneration outcomes. The incorporation of titanium into PCL scaffolds appears to markedly enhance osteogenesis, as evidenced by the elevated densitometric parameters. These results are in concordance with existing literature advocating for the use of composite scaffolds to overcome the limitations of single-material constructs in bone tissue engineering[26].

4. Conclusions

In conclusion, the incorporation of bilayer titanium into polycaprolactone scaffolds significantly enhances bone regeneration compared to bilayer porous PCL alone or CNTR groups. The bilayer porous TiPCL group exhibited higher densitometric parameters, including elevated maximum and mean HU values, as well as increased total HU, indicating enhanced mineralization and scaffold integration. These findings suggest that the addition of titanium to polycaprolactone scaffolds provides a more conducive environment for bone healing, leading to improved structural integrity and tissue regeneration over the 12-month observation period.

6. References

1. Tong Y, Yuan J, Li Z, et al. **Drug-Loaded Bioscaffolds for Osteochondral Regeneration**. *Pharmaceutics* 2024; 16: 1095.
2. Du J, Zhu Z, Liu J, et al. **3D-printed gradient scaffolds for osteochondral defects: Current status and perspectives**. *IJB* 2024; 9: 724.
3. Choe R, Devoy E, Jabari E, et al. **Biomechanical Aspects of Osteochondral Regeneration: Implications and Strategies for Three-Dimensional Bioprinting**. *Tissue Engineering Part B: Reviews* 2022; 28: 766–788.
4. Goga T, Goxha B, Crovace AM, et al. **Tomographic Assessment of Bone Regeneration in Osteochondral Lesion Treated with Various Biomaterials in a Sheep Model Study**. *JFB* 2025; 16: 120.
5. Walker-Bone K. **Regular review: Medical management of osteoarthritis**. *BMJ* 2000; 321: 936–940.
6. Crovace AM, Giancamillo AD, Gervaso F, et al. **Evaluation of in Vivo Response of Three Biphasic Scaffolds for Osteochondral Tissue Regeneration in a Sheep Model**. *Veterinary Sciences* 2019; 6: 90.
7. G. Jacob, K. Shimomura, N. Nakamura. **Osteochondral Injury, Management and Tissue Engineering Approaches**. *Frontiers in Cell and Developmental Biology*; 8. Epub ahead of print 4 November 2020. DOI: 10.3389/fcell.2020.580868.
8. Flaherty T, Tamaddon M, Liu C. **Micro-Computed Tomography Analysis of Subchondral Bone Regeneration Using Osteochondral Scaffolds in an Ovine Condyle Model**. *Applied Sciences* 2021; 11: 891.
9. Welton KL, Logterman S, Bartley JH, et al. **Knee Cartilage Repair and Restoration: Common Problems and Solutions**. *Clinics in Sports Medicine* 2018; 37: 307–330.
10. Wang M, Xu Y, Cao L, et al. **Mechanical and biological properties of 3D printed bone tissue engineering scaffolds.** *Front Bioeng Biotechnol* 2025; 13: 1545693.
11. Khan AR, Gholap AD, Grewal NS, et al. **Advances in smart hybrid scaffolds: A strategic approach for regenerative clinical applications**. *Engineered Regeneration* 2025; 6: 85–110.
12. Dwivedi R, Kumar S, Pandey R, et al. **Polycaprolactone as biomaterial for bone**

scaffolds: Review of literature. *Journal of Oral Biology and Craniofacial Research* 2020; 10: 381–388.

13. De Mori A, Karali A, Daskalakis E, et al. **Poly-ε-Caprolactone 3D-Printed Porous Scaffold in a Femoral Condyle Defect Model Induces Early Osteo-Regeneration**. *Polymers* 2023; 16: 66.
14. Crovace AM, Lacitignola L, Forleo DM, et al. **3D Biomimetic Porous Titanium (Ti6Al4V ELI) Scaffolds for Large Bone Critical Defect Reconstruction: An Experimental Study in Sheep**. *Animals* 2020; 10: 1389.
15. De Wild M, Schumacher R, Mayer K, et al. **Bone Regeneration by the Osteoconductivity of Porous Titanium Implants Manufactured by Selective Laser Melting: A Histological and Micro Computed Tomography Study in the Rabbit**. *Tissue Engineering Part A* 2013; 19: 2645–2654.
16. Khan AR, Grewal NS, Jun Z, et al. **Raising the Bar: Progress in 3D-Printed Hybrid Bone Scaffolds for Clinical Applications: A Review**. *Cell Transplant* 2024; 33: 09636897241273562.
17. Sosio C, Di Giancamillo A, Deponti D, et al. **Osteochondral Repair by a Novel Interconnecting Collagen–Hydroxyapatite Substitute: A Large-Animal Study.** *Tissue Engineering Part A* 2015; 21: 704–715.
18. Hounsfield GN. **Computed Medical Imaging**: *Journal of Computer Assisted Tomography* 1980; 4: 665–674.
19. Bolus D, Morgan D, Berland L. **Effective use of the Hounsfield unit in the age of variable energy CT**. *Abdom Radiol* 2017; 42: 766–771.
20. Pauwels R, Jacobs R, Singer SR, et al. **CBCT-based bone quality assessment: are Hounsfield units applicable?** *Dentomaxillofacial Radiology* 2015; 44: 20140238.
21. Hunter LE, Lubin N, Glassman NR, et al. **Comparing Region of Interest versus Voxel-Wise Diffusion Tensor Imaging Analytic Methods in Mild and Moderate Traumatic Brain Injury: A Systematic Review and Meta-Analysis.** *J Neurotrauma* 2019; 36: 1222–1230.
22. Tukey JW. **Comparing Individual Means in the Analysis of Variance**. *Biometrics* 1949; 5: 99.
23. Kim H-Y. **Statistical notes for clinical researchers: *post-hoc* multiple comparisons**. *Restor Dent Endod* 2015; 40: 172.
24. Lu Y, Wang X, Chen H, et al. **"Metal-bone" scaffold for accelerated peri-implant endosseous healing.** *Front Bioeng Biotechnol* 2024; 11: 1334072.
25. Ramírez-Ruiz F, Núñez-Tapia I, Piña-Barba MC, et al. **Polycaprolactone for Hard Tissue Regeneration: Scaffold Design and In Vivo Implications**. *Bioengineering* 2025; 12: 46.
26. Gharibshahian M, Salehi M, Beheshtizadeh N, et al. **Recent advances on 3D-printed PCL-based composite scaffolds for bone tissue engineering**. *Front Bioeng Biotechnol* 2023; 11: 1168504.